Accepted Article

Title: Protein surface mimetics: understanding how ruthenium tris(bipyridines) interact with proteins

Authors: Sarah H Hewitt; Maria H Filby; Ed Hayes; Lars T Kuhn; Arnout P. Kalverda; Michael E Webb; Andrew John Wilson

Protein surface mimetics: understanding how ruthenium *tris*(bipyridines) interact with proteins

Sarah H. Hewitt, Maria H. Filby, Ed Hayes, Lars T. Kuhn, Arnout P. Kalverda, Michael E. Webb and Andrew J. Wilson*

Abstract: Protein surface mimetics achieve high affinity binding by exploiting a scaffold to project binding groups over a large area of solvent exposed protein surface to make multiple co-operative non-covalent interactions. Such recognition is a pre-requisite for competitive/ orthosteric inhibition of protein-protein interactions (PPIs). This paper describes biophysical and structural studies on ruthenium(II) *tris(*bipyridine) surface mimetics that recognize cytochrome (cyt) *c* and inhibit the cyt c/ cyt *c* peroxidase (CCP) PPI. Binding is electrostatically driven, with enhanced affinity achieved through enthalpic contributions thought to arise from the ability of the surface mimetics to make a greater number of non-covalent interactions with surface exposed basic residues on cyt *c* in comparison to CCP. High field natural abundance ^{1}H-^{15}N HSQC NMR experiments are consistent with surface mimetics binding to cyt *c* in similar manner to CCP. This provides a framework for understanding recognition of proteins by supramolecular receptors and informing the design of ligands superior to the protein partners upon which they are inspired.

Introduction

Protein-protein interactions (PPIs) are considered difficult to inhibit using conventional synthetic molecules;[1,2] they typically involve large interfaces with few discernable pockets on either partner that represent the hallmark of traditional ligandable[3] proteins.[4] Given conventional approaches for ligand discovery e.g. high-throughput screening and fragment based drug discovery have met with limited success in identifying PPI inhibitors,[5,6] supramolecular chemical biology[7] with a focus on understanding and controlling molecular recognition is well placed to elaborate new strategies. One such strategy is the surface mimetic approach;[8–10] protein surface mimetics are a class of molecular structure that utilize a scaffold to project multiple binding groups over a large area of protein surface and achieve high affinity protein binding. Several different scaffolds have been used as protein surface mimetics, including calixarenes,[11–15] porphyrins,[8,16–18] dendrimers,[19–23] metal complexes,[9,24,25] nanoparticles,[26–28] and others.[29–33]

[a]   Miss S. H. Hewitt , Dr M. H. Filby, Dr E. Hayes Dr M. E. Webb Prof A. J. Wilson
       School of Chemistry
       University of Leeds
       Woodhouse Lane, Leeds LS2 9JT, UK
       E-mail: A.J.Wilson@leeds.ac.uk,
[b]   Miss S. H. Hewitt , Dr M. H. Filby, Dr E. Hayes, Dr L. T. Kuhn, Dr A. P. Kalverda Dr M. E. Webb Prof A. J. Wilson
       Astbury Centre For Structural Molecular Biology,
       University of Leeds
       Woodhouse Lane, Leeds LS2 9JT, UK

       Supporting information for this article is given via a link at the end of the document.
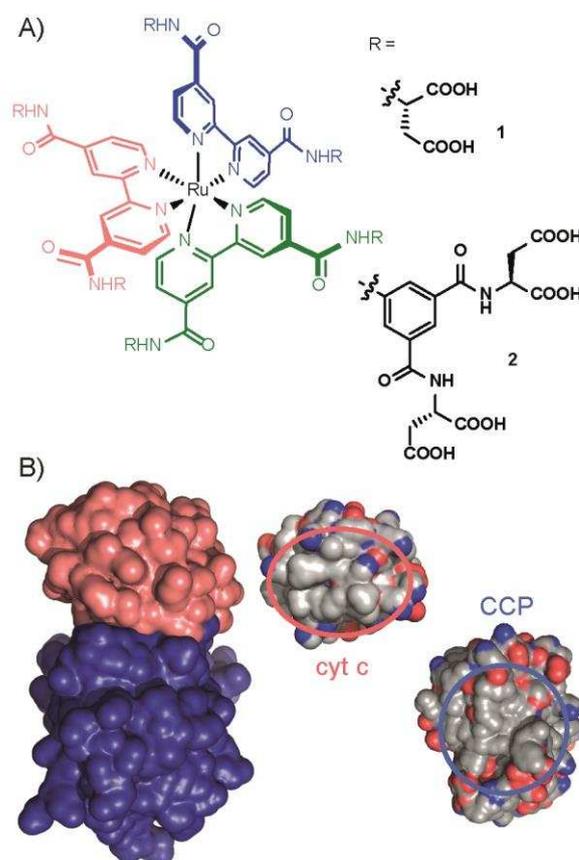
Figure 1. The Ru(II)(bpy)$_3$ surface mimetics and their PPI counterparts, cyt *c* and CCP (A) Ru(II)(bpy)$_3$ complexes **1** and **2,** (B) **t**he cyt *c*/ CCP interaction, cyt *c* in red, CCP in purple (PDB ID 1U75)[34] and (C) the interaction faces of cyt *c* (left) and CCP (right), showing a ring (red circle) of basic amino acid residues (blue) on cyt *c* and a complementary patch (blue circle) on CCP with acidic amino acid residues (red)

We and others previously introduced highly functionalized ruthenium(II) *tris*(bipyridine) (Ru(II)(bpy)$_3$) complexes as protein surface mimetics.[35–41] These large, multivalent, luminescent molecules have a chemically inert core, which can be peripherally functionalized with different binding groups in a stereochemically and geometrically rich manner. Hamachi and coworkers initially designed a carboxylate functionalized Ru(II)(bpy)$_3$ complex capable of binding to cytochrome (cyt) *c* and mediating photoreduction.[35] Subsequently our group and the Ohkanda group designed high affinity Ru(II)(bpy)$_3$ complexes for binding to cyt *c* and α-chymotrypsin.[36–42] In our initial study of five different Ru(II)(bpy)$_3$ complexes, two carboxylic acid functionalized complexes (Figure 1A, complex **1** and **2**) were shown to recognize cyt *c* with nanomolar affinity and do so selectively over acetylated cyt *c* and four other proteins.[36] Complex **2** was also shown to destabilize cyt *c*.[39] Analysis of Ru(II)(bpy)$_3$ complexes with 5'-monosubstituted
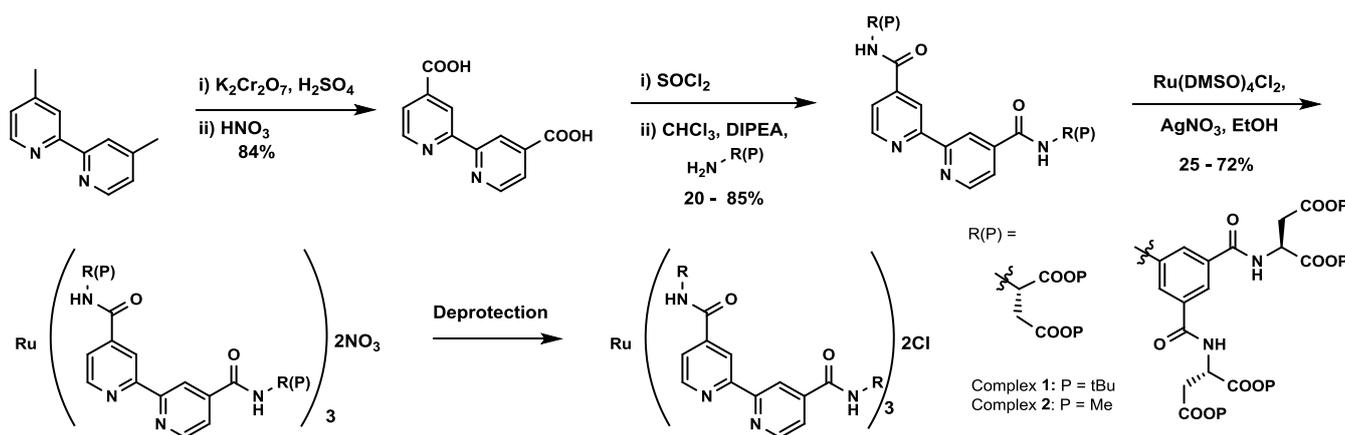
Scheme 1. Synthesis of the Ru(II)(bpy)₃ complex

bipyridine ligands showed a difference in binding affinity between *fac* and *mer* isomers (172 nM versus 25 nM for Δ-isomers respectively), but little difference between Δ and Λ isomers (25 nM versus 29 nM for *mer* isomers respectively), establishing that geometrical shape affects binding.[37] The Ohkanda group used heteroleptic complexes to propose that four of the six arms of Ru(II)(bpy)₃ complexes bearing bpy groups with two substituents interact with cyt *c*.[41] Further studies have shown that these complexes are able to enter cells, with little cytotoxicity.[38,41]

These prior strategies employed a rudimentary design that exploits charge complementarity with the cyt *c* surface;[36,37,43] multiple carboxylic acids are present in order to complement surface exposed basic residues on cyt *c*. However evidence of PPI inhibition,[26,44] detailed information on the nature of binding and any structural information are lacking, which is characteristic of all but a few studies on protein surface recognition using classic supramolecular scaffolds.[18,45,46] Inhibited ascorbate reduction of cyt *c*,[36,37] is consistent with binding to the CCP binding site i.e. the haem-exposed edge of cyt *c*, where there is a hydrophobic patch surrounded by a ring of basic amino acid residues.[47] Herein, we show that highly functionalized Ru(II)(bpy)₃ complexes inhibit the cyt *c*/ CCP interaction and do so through electrostatically and entropically driven binding of cyt *c* in a manner that replicates the binding of cyt *c* by CCP. Higher affinity Ru(II)(bpy)₃ complexes achieve additional potency through enthalpic effects. Finally, using high field NMR we demonstrate that recognition occurs at the haem exposed edge and hence PPI inhibition is orthosteric. Collectively, this provides a more rational framework for the design of supramolecular receptors for cyt *c* and protein-surfaces more widely.

Results and Discussion

Synthesis

Ru(II)(bpy)₃ synthesis proceeds *via* the route shown in Scheme 1, using a *tert*-butyl ester or methyl ester protecting group strategy for complex **1** or **2** respectively. In this generic route, the ligand is first assembled by amide bond formation, *via* a

water sensitive acid chloride, with subsequent complexation using Wilkinson's reagent.[48] The protected complex formed can be purified *via* conventional silica flash column chromatography. Subsequent deprotection with TFA or LiOH affords complexes **1** and **2** respectively. Deprotection of the larger complex **2** requires mild conditions and careful reaction monitoring due to the lability of the anilide bond under both basic and acidic conditions.

Complex 2 inhibits the cyt c/ CCP PPI
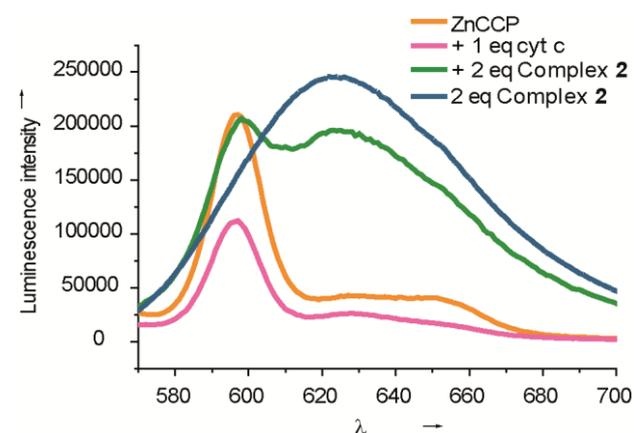
Figure 2. Complex **2** inhibits the cyt c/CCP PPI (A) luminescence data (λ_{ex} = 430 nm, 2 μM ZnCCP (orange), + **2** μM cyt *c* (pink) shows loss of λ_{max} at 595 nm, + 2 μM cyt c and 4 μM **2** (green) shows recovery of λ_{max} at 595 nM and reduced λ_{max} at 625 nM relative to 4 μM **2** alone (blue)

Given that the affinity of complex **2** for cyt *c* which we previously reported,[36] is greater than that of CCP for cyt *c*[49] we anticipated **2** would be a potent inhibitor of the cyt *c*/ CCP interaction. A luminescence quenching assay was implemented (Fig. 2) wherein the luminescence emission from Zn-protoporphyrin substituted CCP[50] is first quenched upon interaction with cyt *c* and then recovered upon displacement with the ruthenium complex. Signal overlap with the Ru(II)(bpy)₃ luminescence (λ_{max}~625 nm) complicates interpretation, however simultaneous loss of MLCT luminescence is observed

relative to the complex in the absence of cyt *c*. A native agarose gel supports successful PPI inhibition (see ESI, Fig. S1).

Binding is Entropically favourable and electrostatic in nature.
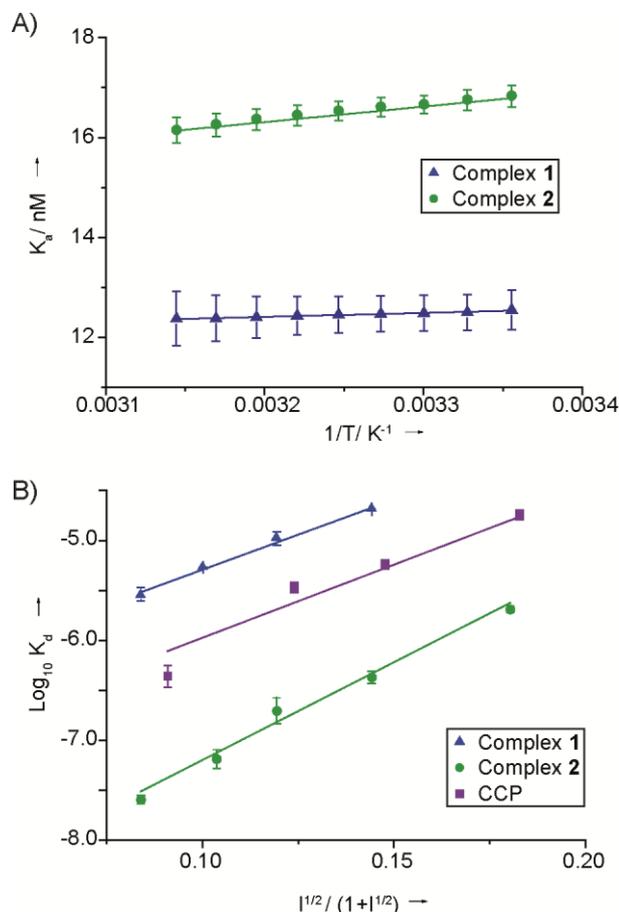
Figure 3. Van't Hoff and Debye-Hückel analysis on the binding interactions between cyt *c* and complexes **1** and **2**, (a) Representative van't Hoff analysis, binding in 5 mM sodium phosphate, 0.2 mg mL^{-1} BSA, pH 7.5, temperature range 25 to 45 ℃, (errors in curve fitting for a single replicate are shown) (b) Debye-Hückel analysis, using the Güntelberg approximation, binding in 5 mM sodium phosphate, 0.2 mg mL^{-1} BSA, pH 7.5, and variable concentrations NaCl, (variation in K_d from two replicates is shown)

The binding affinities of complexes **1** and **2** towards cyt *c* were measured using a luminescence quenching assay,[36] where the luminescence of the ruthenium complexes is quenched on binding to cyt *c* through photoinduced electron transfer to its haem group. Previously, cuvette-based fluorescence was used for binding studies,[36,37] however optimization of the assay on a 384 well plate was required for higher-throughput screening of the binding under different conditions. Addition of a blocking agent, bovine serum albumin (BSA), was found to be required to allow for agreement between the two methods. The addition of BSA accompanied a concurrent decrease in binding affinity (from K_d 10.5 ± 0.4 nM to 42.9 ± 3.1 nM for complex **2**) (See ESI Fig. S1). Determination of K_d at different temperatures and subsequent van't Hoff analyses (Figure 3A) provided thermodynamic parameters (Table 1) for binding (Equation 1),

making the assumption that ΔH and ΔS are temperature-independent

$$lnK_a = -\Delta H/RT + \Delta S/R \qquad \text{Eq. 1}$$

These data show that for complex **1** binding to cyt *c* is primarily driven by entropic contributions with a small favorable enthalpic contribution, whereas for complex **2** it is both entropically and enthalpically driven. In comparison the cyt c/ CCP interaction is entropically driven, and enthalpically is mildly unfavourable.[49] Thus, complex **1,** with fewer carboxylates, more closely matches the thermodynamic profile of CCP in binding to cyt *c*. A plausible hypothesis for enhanced binding of complex **2** to cyt *c*, is that the additional carboxylic acids form increased numbers of salt bridges with the basic amino acids on the cyt *c* surface.

Table 1. Thermodynamic parameters derived from the van't Hoff analysis for the binding of complexes **1** and **2** to cyt *c* (errors derived from triplicate experiments), and literature values for the cyt *c*/CCP interaction under similar conditions[49]

	Complex 1	Complex 2	CCP[49]
ΔH / kJ mol^{-1}	-6.6 ± 0.4	-26.3 ± 3.0	9.4 ± 0.8
TΔS (25 °C) / kJ mol^{-1}	24.5 ± 0.4	16.0 ± 3.0	38.4 ± 0.9
ΔG (25 °C) / kJ mol^{-1}	-31.0 ± 0.4	-42.3 ± 0.0	-27.9 ± 1.0

Table 2. Binding in variable ionic strengths, 5 mM sodium phosphate, 0.2 mg mL^{-1} BSA, pH 7.5, variable concentration NaCl, nd=not determined

Ionic strength/ mM	Complex 1 K_d / μM	Complex 2 K_d/ nM
8.39	2.88 ± 0.46	25.3 ± 2.4
13.39	4.25 ± 0.47	64.8 ± 13.7
18.39	10.30 ± 1.61	196.5 ± 59.2
28.39	20.23 ± 0.16	426.5 ± 59.8
48.39	nd	2040.9 ± 152.6

To further understand the electrostatic contribution to binding, affinities were determined at different ionic strength (I). Cyt *c* binding by both complex **1** and **2** is highly dependent upon ionic strength (Table 2), with binding affinity decreasing on increasing ionic strength, suggesting electrostatics dominate binding. The K_d values could be fit to the Debye-Hückel relationship (Eq. 2) (Figure 3(B)), in this case using a Güntelberg approximation (Eq. 3), which is valid up to I = 100 mM.

$$\log K_A = \log K_A^0 - 0.509 Z_1 Z_2 \mu \qquad \text{Eq. 2}$$
$$\mu \approx \sqrt{(I)}/(1+\sqrt{I}) \qquad \text{Eq. 3}$$

From this relationship the parameters K_d^0 and Z_1Z_2 can be established (Table 3), providing an estimate of the affinity at I = 0 and the product of the interacting positive and negative charges. The data were consistent with the Güntelberg approximation for both complexes (Figure 3B), and the calculated values of K_d^0 show high affinity binding for complex **2** and weaker binding for complex **1** at zero ionic strength. The product, Z_1Z_2, provides an indication of the charges involved in the interaction, with complex **2** having a larger value than complex **1** and CCP. Using these data, the charge on the complex interacting with cyt *c* can be estimated. A rudimentary interpretation of this date is made possible by assuming that cyt *c* has the same charge in all cases (calculated to be ~6 at pH 7.5);[51] the charge on complex **1**, **2** and CCP can thus be

calculated as 4.3, 5.9 and 4.8, respectively. Complex **1** and CCP have relatively similar charges, suggesting they make similar electrostatic interactions with cyt *c*. Complex **2** has a larger charge indicating increased electrostatic interactions with cyt *c*. This is consistent with the van't Hoff analyses. Accounting for the crudeness of the Debye-Hückel approximation where small (~3 Å), evenly dispersed charges are assumed (even when using the Güntelberg extension), the data indicate that perhaps not all carboxylates are deprotonated under the assay conditions (i.e. pH 7.4) and/or that a limited number of carboxylates are needed for productive protein surface recognition (even fewer than the number identified in the "deletion" study by the Ohkanda group using heteroleptic complexes),[41]

Table 3. Parameters derived from the Güntelberg approximation of Debye-Hückel analysis for the binding of complexes **1** and **2** to cyt c and literature values for CCP in similar conditions[52]

	Complex 1	Complex 2	CCP[52]
K_d^0 / nM	253 ± 5	1.11 ± 0.21	40.7 ± 23.0
$Z_1 Z_2$	25.9 ± 1.9	35.6 ± 1.3	28.8 ± 4.8

Table 4. Binding affinities for complex 2 to cyt c in different buffers. All buffers were at 5 mM concentration, pH 7.5

Buffer	K_d / nM
Sodium phosphate	42.9 ± 3.1
Potassium phosphate	26.2 ± 3.1
MOPS	35.2 ± 3.1
HEPES	31.2 ± 3.1
Tris	106.3 ± 32.6
btp	133.5 ± 37.4

Differences in affinity between cyt *c* and complex **2** were also studied in different buffers (Table 4). Variation in affinity might discriminate different contributions to binding as negatively charged anions must be displaced from cyt *c* and positively charged cations from complex **2**. In potassium and sodium phosphate no difference in affinity between complex **2** and cyt *c* is observed, indicating interaction of the cationic buffer components with complex **2** are not significant. For binding of cyt *c* to complex **2** in phosphate or sulfonic acid buffers (MOPS and HEPES), similar affinities are also observed. This suggests the nature of the anion and, more importantly, hydrophobicity of the buffer are not significant in mediating molecular recognition, and, reinforce the conclusions gleaned from Debye-Hückel analysis that the interaction is dominated by electrostatic contributions. For the *tris* buffers (*btp* and *tris*) a small decrease in binding affinity is observed. Although a difference in behavior due to the counter chloride anion cannot be excluded, this may be due to the ability of *btp* and *tris* to make different interactions with both cyt *c* and complex **2**; in addition to the ammonium function, the hydroxyls on the buffer may make chelating hydrogen-bonds with charged residues on either.

Cyt *c* is a stable protein that does not unfold over a wide range of pHs, however its ionization state is affected by pH,[53]

hence the pH of the solution was expected to affect recognition of cyt *c* by Ru(II)(bpy)$_3$ complexes. To investigate the binding affinity between complex **2** and cyt *c* over a broad pH regime, *btp* was used as it allows for a pH range of 6.5–9.5. The affinity follows an inverted bell shaped profile (Figure 4A), which maps reasonably well onto the ionization state of cyt *c* (Figure 4A inset).[53] The affinity between pH 7.0–8.5 is relatively constant with decreased binding observed at pH 6.5 and pH 9.0. Residues that become protonated/deprotonated in this pH regime are His-33 and Lys-79 respectively.[53] Lys-79 (green) is at the haem exposed edge (Figure 4B) where binding of complex **2** is thought to occur, whereas His-33 (pink) is on the distal face of cyt *c*. A number of reasons for a decrease in binding affinity at this pH are possible: (a) complex **2** binds to a different or multiple sites on cyt *c*, (b) binding of complex **2** causes subtle conformational changes that transmit to the distal face of cyt *c* affecting the pK_a of His-33, (c) protonation of His-33 causes subtle conformational changes that affect binding interactions on the haem exposed edge, or (d) the protonation state of complex **2** is changed at pH 6.5. More careful analysis of the pH-K_d/ionization state profiles reveals a discrepancy. The ionization state of cyt *c* drops at pH 8.0 rather than pH 8.5 where the binding diminishes, suggesting that binding of complex **2** might mask Lys-79 and increase its pK_a. In contrast there is no difference in the profiles for K_d and ionization state of cyt *c* in the lower pH range suggesting that the pK_a of His-33 is not affected by binding and that loss of affinity more likely derives from a change in ionization state on complex **2**.
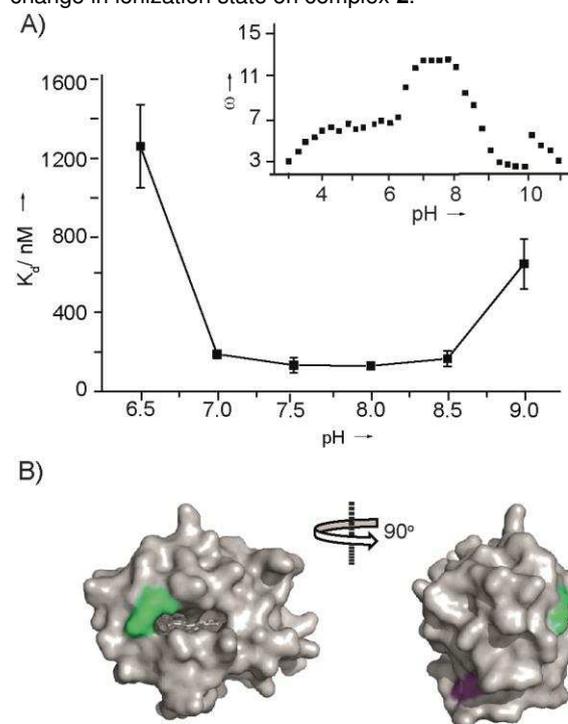

Figure 4. Effect of pH on the binding of complex **2** to cyt *c*. (a) Binding affinity over the range pH 6.5 – 9.0, inset the electrostatic interaction factor (ω) of cyt c over a range of pHs (base limb of titration curve)[53], (b) Cyt c structure (PDB ID 1U75)[54] with residues that become protonated at pH 6.5 and 9.0, His-33 (pink) and Lys-79 (green) respectively
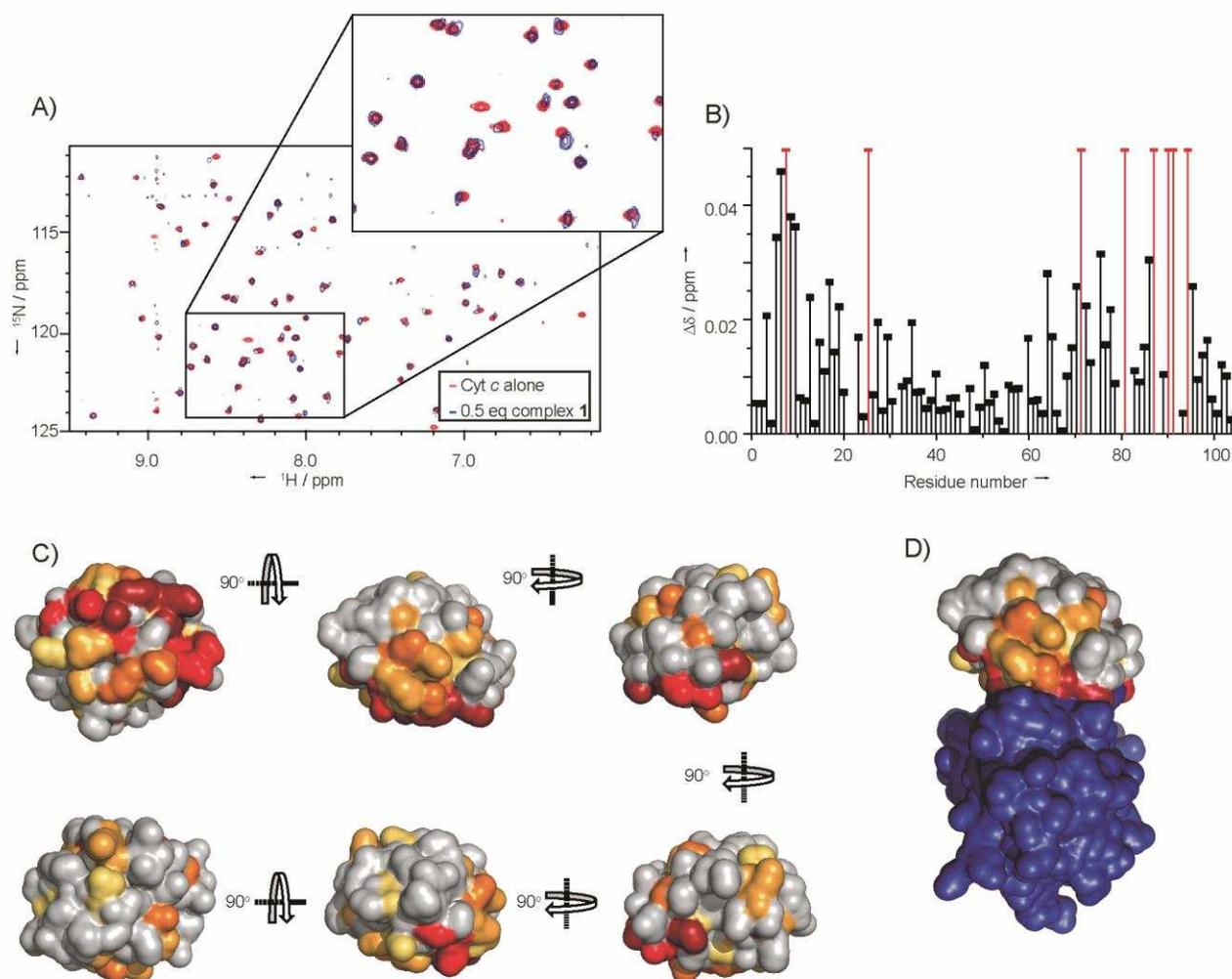
Figure 5. ^{1}H-^{15}N HSQC NMR data of complex **1** binding to cyt *c*. (A) Region of the overlaid HSQC spectrum of cyt *c* (red) and cyt *c* with 0.5 eq complex **1** (blue), Inset shows zoom in of part of the spectrum, showing some peaks staying the same, some having shifted and one disappearing. (B) ^{1}H-^{15}N chemical shift differences ($\Delta\delta$) for the different amino acid residues with and without complex **1**. Gaps are for prolines and unassigned amino acids, red bars show amino acids for which the signal disappears due to significant line-broadening of NH cross-peaks on addition of complex **1**. (C) Chemical shift perturbation map of cyt c, molecular surface of cyt c generated from PyMol (PDB ID 1U75),[54] with coloring corresponding to the extent of chemical shift changes ($\Delta\delta$) on addition of the complex. Amino acids with ^{15}N-^{1}H resonances that disappear in dark red, exhibit large chemical shift changes ($\Delta\delta > 0.03$) in red, moderate changes ($\Delta\delta > 0.02$) in orange, small changes ($\Delta\delta > 0.015$) in yellow-orange and very small chemical shift changes ($\Delta\delta > 0.01$) in yellow. (D) perturbation map of cyt c (as(C)) in complex with CCP (purple), this view corresponds to that of the central top image in Figure 5C, (PDB ID 1U75)[34]

High-Field NMR reveals complexes 1 and 2 bind to the CCP binding site on cyt *c*

While the pH data provide some crude structural information on the cyt *c* binding site of Ru(II)(bpy)₃ complexes, more detailed residue-specific, atomic-level data were sought. To identify the binding site of complex **1** and **2** on cyt *c*, a sensitivity-enhanced natural abundance ^{1}H-^{15}N HSQC spectrum of cyt *c* in the presence and absence of complex **1** was recorded, using a 950 MHz NMR spectrometer. 2 mM sodium ascorbate was added to the buffer, to reduce the iron in cyt *c* from paramagnetic Fe(III) to diamagnetic Fe(II), thus minimizing its influence on the spectrum, i.e. paramagentic line broadening. The binding of the complexes to cyt *c* for reduced versus oxidized cyt *c* is similar (for complex **2**, K_d = 92.4 ± 5.5 and 49.6 ± 13.3 nM respectively, in 5 mM phosphate, 2 mM sodium ascorbate, 0.2 mg mL^{-1} BSA).

The assignment of the ^{1}H-^{15}N HSQC spectrum of horse heart cyt *c* has previously been obtained.[55] Upon addition of

complex **1**, the NMR data show several cross-peaks having disappeared, while others display chemical shift changes ranging from 0.015-0.05 ppm indicating the presence of protein-ligand interactions (Figure 5A and 5B). When these chemical shift changes are mapped onto the structure of cyt *c* from the cyt *c*/ CCP crystal structure,[54] the data indicate binding occurs predominantly to one side of the haem group, with the opposite face having very few amino acids with sizeable shifts in their HSQC peaks (Figure 5C). The binding site is in a similar location to that of carboxylic acid functionalized porphyrins.[18] In comparison to the cyt *c*/ CCP interaction (Figure 5D), it can be seen that the amino acids whose cross-peaks have shifted are in and around the PPI interface, indicating complex **1** is an effective mimic of CCP, binding at the same face and capable of acting as an orthosteric inhibitor of the interaction.

Attempts to acquire data in the presence of complex **2** were difficult due to the high affinity binding and the relatively high concentrations required for natural abundance NMR. At 1:1 ratios of cyt *c* and complex **2**, data could not be obtained due to

the formation of oligomers and a concomitant loss of NMR signal intensity, caused by significant line-broadening.This unsurprising to us as given the potential for aggregation at higher concentrations and the observation of additional binding modes in NMR studies using porphyrins.[18] Further evidence of an additional/alternative binding mode for the larger complex **2**, is the visualization of a second binding event for complex **2** with yeast cyt *c*, but a single binding event for complex **1** (See ESI, Fig. S2). Even at 1:2 equivalents complex **2**:cyt *c* multiple signals disappeared, so detailed information as to the binding site could not be gleaned, however of the signals present, chemical shift changes were detected for regions of the protein backbone located on the same binding face as for complex **1**, and on the haem exposed edge.

Conclusions

We have performed a detailed study on the cyt *c* binding properties of two synthetic Ru(II)(bpy)$_3$ complexes **1** and **2**. The ruthenium complexes are potent ligands for selective protein surface recognition of cyt *c* and capable of inhibiting the cyt *c*/ CCP PPI. Binding is shown to be entropically favorable and driven by complementary electrostatic interactions between the basic protein and acidic Ru(II)(bpy)$_3$ complexes. This profile is consistent with accurate mimicry of the cyt *c* binding properties of CCP. Higher-affinity recognition of the protein target can be achieved through the addition of further acidic motifs on the Ru(II)(bpy)$_3$ complexes allowing additional enthalpically favorable electrostatic interactions to occur. Finally, NMR experiments establish that the Ru(II)(bpy)$_3$ complexes **1** and **2** bind to the solvent exposed cyt *c* surface further underscoring the ability of the complexes to act as mimics of CCP and confirming an orthosteric mode of PPI inhibition. These studies highlight the value of detailed analyses of protein-surface recognition by supramolecular hosts in terms of rationalizing structure function relationships, and informing subsequent designs. Moreover the conclusions of this study point to a future need for syntheses/ assembly of asymmetrically functionalized Ru(II)(bpy)$_3$ complexes to maximize productive protein-ligand contacts and selectivity of protein surface recognition. This and the application of our approach to therapeutically attractive protein targets will form the basis of future studies by our group.

Experimental Section

Synthesis

Synthesis was adapted from literature.[36] A representative synthesis of complex **1** is shown below. The synthesis of complex **2** is described in the supplementary information.

(2S,2'R)-tetra-*tert*-butyl-2,2'-(([2,2'-bipyridine]-4,4'-dicarbonyl)bis (azanediyl)) disuccinate

2,2'-bipyridine-4,4'-dicarboxylic acid (100 mg, 0.400 mmol), triethylamine (1 drop) and thionyl chloride (4 mL) were heated under reflux for 16 hours. The mixture was cooled to room temperature and the thionyl chloride removed *in vacuo* to yield the acid chloride as an orange-red

solid. The dry acid chloride was then redissolved in dry chloroform (20 mL) and added dropwise to a stirred solution of di-*tert* butyl L-aspartic acid.HCl (253 mg, 0.901 mmol) and triethylamine (0.25 mL, 1.80 mmol) in dry chloroform at 0 °C. The reaction mixture was warmed to room temperature and refluxed for 48 hours. The mixture was cooled to room temperature and the solvent removed to yield the crude product as a brown oil. This was purified by flash column chromatography (3 % - 6 % MeOH in CHCl$_3$) to yield the product as a yellow solid (262 mg, 0.375 mmol, 91 %); ^{1}H NMR (300 MHz, CDCl$_3$) δ ppm 1.49 (s, 18 H, H1/H2), 1.52 (s, 18 H), 2.91 (dd, *J*=17.2, 4.3 Hz, 2 H), 3.04 (m, *J*=17.2, 4.3 Hz, 2H), 4.92 (dt, *J*=7.5, 4.3 Hz, 2 H), 7.46 (d, *J*=7.5 Hz, 2 H), 7.77 (dd, *J*=5.0, 1.65 Hz, 2 H), 8.78 (app. s, 2 H), 8.83 (d, *J*=5.0 Hz, 2 H); ^{13}C NMR (126 MHz, CDCl$_3$) δ ppm 28.0, 28.1, 37.5, 49.7, 81.9, 82.8, 118.0, 121.8, 142.3, 150.1, 156.3, 165.1, 169.5, 170.2 ; IR (solid state) 3346, 2975, 2928, 1723, 1650; ESI-HRMS: found *m/z* 699.3615, [C$_{36}$H$_{51}$N$_4$O$_{10}$]$^+$ requires 699.3599

Tris ((2S,2'R)-tetra-*tert*-butyl-2,2'-(([2,2'-bipyridine]-4,4'-dicarbonyl)bis (azanediyl))disuccinate) ruthenium(II) dinitrate

(2S,2'R)-tetra-*tert*-butyl-2,2'-(([2,2'-bipyridine]-4,4'-dicarbonyl)bis (azanediyl)) disuccinate (300 mg, 0.429 mmol), (dimethylsulfoxide)dichlororuthenium (II) (65 mg, 0.134 mmol), silver nitrate (46 mg, 0.268 mmol) and ethanol (20 mL) were heated under reflux for 7 days. After which time the reaction mixture was filtered hot and concentrated. The red solid was then loaded onto an SP Sephadex column and eluted with 1:1 acetone: 0.1 M NaCl solution and all the red fractions collected and concentrated. The combined red fractions were redissolved in acetone and filtered to remove sodium chloride, and this was repeated until no more white salt was visible in the concentrated sample. The complex was then purified by flash chromatography (1 – 3 % MeOH in CHCl$_3$) and the red fractions collected. These were concentrated, redissolved in CHCl$_3$ and extracted with water to yield the product as a red solid (77 mg, 0.034 mmol, 25 %); ^{1}H NMR (300 MHz, Acetone) δ ppm 2.10 (app s, 108 H), 2.81 - 3.07 (m, 24 H), 4.79 - 5.07 (m, 24 H), 7.89 (dd, *J* = 15.8, 6.6 Hz, 12 H), 8.37 (dd, *J* = 15.8, 8.5 Hz, 12 H), 8.82 - 8.98 (m, 12 H); ^{13}C NMR (126 MHz, CDCl$_3$) δ ppm 27.9, 28.1, 29.6, 37.1, 50.9, 81.4, 82.4, 123.5, 143.5, 157.2, 157.3, 162.2, 169.2, 169.4, 170.0; ESI-HRMS: found *m/z* 1098.4854, [C$_{108}$H$_{150}$N$_{12}$O$_{30}$Ru]$^{2+}$ requires 1098.4822; λ$_{max}$ (MeOH): 306 nM (ε/ dm^3 mol^{-1} cm^{-1} 240 723 981)

Tris (2S,2'R)-2,2'-(([2,2'-bipyridine]-4,4'-dicarbonyl)bis (azanediyl))disuccinicacid) ruthenium(II) ditrifluoroacetate, complex 1

Tris ((2S,2'R)-tetra-*tert*-butyl -2,2'-(([2,2'-bipyridine] -4,4'-dicarbonyl) bis(azanediyl)) disuccinate) ruthenium(II) dinitrate(68 mg,), TFA (4.5 mL) and water (0.5 mL) were stirred for 3 days. The reaction mixture was then concentrated *in vacuo* to yield the product as a red-black solid (57 mg, 0.0294 mmol, 98 %); ^{1}H NMR (500 MHz, D$_2$O) δ ppm 8.97 (s, 1 H), 7.90 (s, 1 H), 7.70 (s, 1 H), 4.61 (s, 1 H), 2.78 (s, 1 H), 2.67 (s, 1 H'), ; IR (solid state) 3182, 3050, 1648; ESI-HRMS: found *m/z* 762.1081, [C$_{60}$H$_{54}$N$_{12}$O$_{30}$Ru]$^{2+}$ requires 762.1056;

Protein Expression and Purification

Cytochrome *c* peroxidase (CCP) was overexpressed in *Escherichia coli* (*E. coli*) using the plasmid pT7CCP) in which expression was placed under the control of T7 RNA polymerase. The enzyme was isolated from *E. coli* BL21 (DE3) as an apo-enzyme which was purified according to the literature.[1]. A 2 L culture of the expression strain supplemented with ampicillin was grown at 37 °C for 36 h in a medium containing (per litre) 10 g of bactotryptone, 8 g of yeast extract, 5 g of NaCl, 1 mL of glycerol, and 100 mg of ampicillin. Subsequent steps were performed at 4 °C. The cells were harvested by centrifugation at 6000*g* for 10 min, resuspended

in 40 mL of buffer containing 200 mM potassium phosphate pH 7.5, 2 tablets of Roche protease inhibitor tablets mini, and 1 mM EDTA, and lysed by passing through a cell disrupter. The lysate was diluted with 100 mL of cold H_2O. Enough ascorbic acid was added to bring the buffer to 5mM. To improve the ratio of the soret band to the band at 280 nm of FeCCP, an excess of haem was added, 80 mg of haemin/ 12 L culture was dissolved in a minimal amount of 100 mM KOH in the dark, and diluted 10 times with 100 mM potassium phosphate, pH 6. The haem solution was gradually added to clarified lysate on ice over 30 minutes with gentle stirring, then stirred on ice for 1 hour in the dark. The excess haem was then precipitated by first acidifying the solution with 100 mM acetic acid to pH 5.0, and freezing the solution in dry ice until just frozen. The solution was then allowed to just thaw with gentle shaking at 37 °C The solution was centrifuged at 10 000 – 12 000 rpm for 20 minutes and the supernatant decanted. The clear supernatant was loaded onto a DEAE-Sepharose CL-6B (3 x 5 cm) column equilibrated with 50 mM potassium phosphate, pH 6, and washed with the same buffer. After elution with 500 mM potassium phosphate, pH 6, the enzyme-containing fractions were diluted with an equal volume of cold H_2O and concentrated to approximately 1 mL by ultrafiltration (Amicon YM-10 membrane). The sample was centrifuged at 12000g for 2 min to remove insoluble material, loaded onto a Sephadex G-75 superfine column (3 x 60 cm) and eluted with 100 mM potassium phosphate, pH 6, and 1 mM EDTA. The fractions containing A408/A280 >1.1 were pooled (protein concentration was determined from the molar absorptivity; ε = 55 mM^{-1} cm^{-1}, at 282 nm).

In order to exchange the haem for Zn porphyrin, the haem was removed using the acid butanone method[2] with minor modifications. A ~1 mM solution of haem CCP in 100 mM potassium phosphate buffer was diluted with 4 volumes of ice-cold water. The CCP solution was brought to 100 mM fluoride by addition of 1 M KF solution, breaking the haem-protein linkage and turning the solution green. The haem was removed by lowering the pH of the solution to pH 3.2-3.3 by adding ice cold 0.1 M HCl dropwise, with gentle stirring. The haem was then extracted by adding an equal volume of ice cold 2-butanone, shaking for 30 seconds and centrifuged for 1 minute at 1000g. The brown layer was siphoned away and the extraction repeated until the aqueous layer became colourless. The resulting apoCCP solution was diluted with a half volume of cold water and dialysed against 2-3 changes of 10 mM $NaHCO_3$ solution. It was then dialysed against water, changing the outer solution every 2 hours until the bag no longer smelt of butanone (~24 hours), followed by dialysis into 10 mM *Tris*-HCl, pH 7. A 4:1 excess of porphyrin was dissolved in 200-500 µL of 100 mM KOH and diluted 5-10 times with water. The porphyrin solution was added to the protein solution, and the protein solution titrated to pH 7.8 with 100 mM KOH. In the dark, the alkaline porphyrin solution was added dropwise with gentle stirring to apoCCP until ~2 fold excess of porphyrin was present. The solution was left to stand at near pH 8 for 20-30 minutes than brought to pH 6.5-7.0 by addition of 1 M monobasic potassium phosphate. The protein was exchange into 25 mM potassium phosphate, pH 6.5 and concentrated by ultracentrifugation to 0.5-1.0 mM CPP. The protein was loaded onto a small column of DEAE Sepharose CL-6B, pre-equilibrated with 25 mM potassium phosphate, pH 6.5. The column was rinsed with around half a volume of loading buffer, and the metalloporphyrin CCP eluted with 0.6 M potassium phosphate, pH 6.5.

Inhibition of Cyt c/CCP by fluorescence recovery

To a 500 µL micro fluorescence cell (Hellma Analytics) containing 500 µL of 2 µM ZnCCP (ε_{280} = 55 mM^{-1}cm^{-1}) was added 1 eq of cytochrome c, in a solution containing 2 µM ZnCCP. 2 equivalents of complex **2** were then added. Fluorescence spectra where taken at each point (ex. 430 nm). A separate comparative spectra for complex **2** was taken using identical instrument settings

Luminescence quenching assays

All stocks for luminescence intensity assays were made up in 5 mM phosphate buffer (pH 7.5). Ruthenium complex stocks were made up to 2 mM. Horse heart and yeast cyt *c* was obtained from Sigma Aldrich, and used without further purification. A cytochrome *c* stock was made up to ~1 mM, and the concentration accurately determined using the molar extinction coefficient at 550 nm of 2.95×10^4 mol^{-1} dm^3 cm^{-1} for horse heart cyt c [56] and 2.11×10^4 mol^{-1} dm^3 cm^{-1} for yeast cyt c[56] after reduction by addition of one microspatula of sodium dithionite. Assays with oxidized cyt *c* in ascorbate containing buffer used cyt *c* oxidized with $K_3Fe(CN)_6$ followed by dialysis into 5 mM sodium phosphate, 2 mM sodium ascorbate, pH 7.5 buffer, to remove the excess $K_3(CN)_6$. The concentration of oxidized cyt *c* was determined by using the molar extinction coefficient at 410 nm of 1.061×10^5 mol^{-1} dm^3 cm^{-1}[57].All buffers used were at 5 mM concentration, 0.2 mg mL^{-1} BSA, pH 7.5, unless otherwise stated.

Fluorometer luminescence quenching assays were measured on a Jobin-Yvon Spex Fluorolog-3 fluorometer. Measurements were taken in a 4 mL quartz cuvette with excitation at 467 nm and emission measured over the range 575 – 675 nm, with 10 nm slit widths on both excitation and emission. Peak maxima were recorded over the entire cyt *c* concentration gradient.

Plate reader luminescence quenching assays, were performed using a Perkin Elmer EnVision^{TM} 2103 MultiLabel plate reader, with excitation at 467 nm, and emission at 630 nm fixed wavelength. A 2/3 dilution regime in a 384 well plate (Optiplate) was used (total well volume 50 µL), with each result measured in triplicate. The K_d ranges possible for this assay is ~5 nM – ~100 µM

In all assays the ruthenium complex concentration was kept constant, with the concentration of cyt c being varied through the assay, as described below. Results obtained were fitted, using Origin9, to a 1:1 binding isotherm:

$$I = \frac{m[(a+b+K) - \sqrt{(a+b+K)^2 - 4ab}]}{2a}$$

Where *I* = change in relative luminescence intensity (I/I$_0$), m = maximum value of *I*, a = concentration of complex, K = dissociation constant, b = concentration of protein added

Protein NMR

Sensitivity enhanced ^{1}H-^{15}N HSQC NMR correlation spectra of ligand-bound and unbound forms of cyt *c*, purchased from Sigma Aldrich, were carried out at natural abundance using a 950 MHz Bruker Ascend^{TM} Aeon spectrometer operating at a proton (^{1}H) resonance frequency of 950.13 MHz equipped with a Bruker TCI triple-resonance cryo-probe. NMR acquisitions were carried out in 5 mM sodium phosphate, 2 mM sodium ascorbate, pH 7.25 buffer. For cyt *c* alone, spectra were taken at 2 mM protein concentration. With complex **1**, 1 mM cyt c and 0.5 mM complex **1** were used, to a total volume of 600 µL. Spectra were analysed using the CcpNmr Analysis software package and the chemical shift perturbations were calculated as the square root of the sum of the isotope weighted shift differences squared (Eq. 4),

$$\Delta \delta = \sqrt{(\Delta \delta_N)^2 + (^{\gamma_H}/_{\gamma_N})^2 (\Delta \delta_H)^2}$$

where $\Delta \delta$ is the overall change in chemical shift, $\Delta \delta_N$ is the change in the nitrogen dimension and $\Delta \delta_H$ is the change in the proton dimension, respectively. The change in the proton dimension is scaled by the ratio of

the gyromagnetic ratio of ^{15}N (γ_N) and ^{1}H (γ_H) to account for the larger chemical shift range of nitrogen.

Acknowledgments

[1] M. R. Arkin, J. A. Wells, *Nat. Rev. Drug Discov.* **2004**, *3*, 301–17.

[2] A. J. Wilson, *Chem. Soc. Rev.* **2009**, *38*, 3289–300.

[3] F. N. B. Edfeldt, R. H. A. Folmer, A. L. Breeze, *Drug Discov. Today* **2011**, *16*, 284–287.

[4] M. J. Waring, J. Arrowsmith, A. R. Leach, P. D. Leeson, S. Mandrell, R. M. Owen, G. Pairaudeau, W. D. Pennie, S. D. Pickett, J. Wang, et al., *Nat. Rev. Drug Discov.* **2015**, *14*, 475–486.

[5] V. Azzarito, K. Long, N. S. Murphy, A. J. Wilson, *Nat. Chem.* **2013**, *5*, 161–173.

[6] M. R. Arkin, A. Whitty, *Curr. Opin. Chem. Biol.* **2009**, *13*, 284–290.

[7] D. a Uhlenheuer, K. Petkau, L. Brunsveld, *Chem. Soc. Rev.* **2010**, *39*, 2817–2826.

[8] S. Fletcher, A. D. Hamilton, *Curr. Opin. Chem. Biol.* **2005**, *9*, 632–8.

[9] S. H. Hewitt, A. J. Wilson, *Chem. Commun.* **2016**, *52*, 9745–9756.

[10] L. Milroy, T. N. Grossmann, S. Hennig, L. Brunsveld, C. Ottmann, *Chem. Rev.* **2014**, *114*, 4695–4748.

[11] R. Zadmard, N. S. Alavijeh, *RSC Adv.* **2014**, *4*, 41529–41542.

[12] M. A. Blaskovich, Q. Lin, F. L. Delarue, J. Sun, H. S. Park, D. Coppola, A. D. Hamilton, S. M. Sebti, *Nat. Biotechnol.* **2000**, *18*, 1065–70.

[13] H. S. Park, Q. Lin, A. D. Hamilton, *J. Am. Chem. Soc.* **1999**, *121*, 8–13.

[14] Y. Hamuro, M. C. Calama, H. S. Park, A. D. Hamilton, *Angew. Chemie Int. Ed. English* **1997**, *36*, 2680–2683.

[15] R. E. McGovern, H. Fernandes, A. R. Khan, N. P. Power, P. B. Crowley, *Nat. Chem.* **2012**, *4*, 527–33.

[16] D. Margulies, Y. Opatowsky, S. Fletcher, I. Saraogi, L. K. Tsou, S. Saha, I. Lax, J. Schlessinger, A. D. Hamilton, *Chembiochem* **2009**, *10*, 1955–8.

[17] H. Zhou, L. Baldini, J. Hong, A. J. Wilson, A. D. Hamilton, *J. Am. Chem. Soc.* **2006**, *128*, 2421–5.

[18] P. B. Crowley, P. Ganji, H. Ibrahim, *ChemBioChem* **2008**, *9*, 1029–33.

[19] S. Mignani, S. El Kazzouli, M. M. Bousmina, J.-P. Majoral, *Chem. Rev.* **2014**, *114*, 1327–42.

[20] F. Chiba, T. Hu, L. J. Twyman, M. Wagstaff, *Chem. Commun.* **2008**, *4351–4353*, 4351–4353.

[21] H. Azuma, Y. Yoshida, D. Paul, S. Shinoda, H. Tsukube, T. Nagasaki, *Org. Biomol. Chem.* **2009**, *7*, 1700–1704.

[22] D. Paul, H. Miyake, S. Shinoda, H. Tsukube, *Chem. - A Eur. J.* **2006**, *12*, 1328–38.

[23] J. Simpson, Y. Liu, W. A. Goddard, J. Giri, M. S. Diallo, *ACS Nanotechnol.* **2011**, *5*, 3456–3468.

[24] D. Ponader, P. Maffre, J. Aretz, D. Pussak, N. M. Ninnemann, S. Schmidt, P. H. Seeberger, C. Rademacher, G. U. Nienhaus, L. Hartmann, *J. Am. Chem. Soc.* **2014**, *136*, 2008–2016.

[25] D. Grünstein, M. Maglinao, R. Kikkeri, M. Collot, K. Barylyuk, B. Lepenies, F. Kamena, R. Zenobi, P. H. Seeberger, *J. Am. Chem. Soc.* **2011**, *133*, 13957–13966.

[26] H. Bayraktar, P. S. Ghosh, V. M. Rotello, M. J. Knapp, *Chem. Commun. (Camb).* **2006**, 1390–2.

[27] K. Saha, S. S. Agasti, C. Kim, X. Li, V. M. Rotello, *Chem. Rev.* **2012**, *112*, 2739–79.

[28] †,§ Nicholas O. Fischer, § Ayush Verma, § Catherine M. Goodman, § and Joseph M. Simard, †,§ Vincent M. Rotello*, **2003**, DOI 10.1021/JA0352505.

[29] T. Schrader, S. Koch, *Mol. Biosyst.* **2007**, *3*, 241–8.

[30] C. Renner, J. Piehler, T. Schrader, *J. Am. Chem. Soc.* **2006**, *128*, 620–628.

[31] Reza Zadmard, T. Schrader*, *J. Am. Chem. Soc.* **2004**, *127*, 904–915.

[32] A. J. Wilson, J. Hong, S. Fletcher, A. D. Hamilton, *Org. Biomol. Chem.* **2007**, *5*, 276–85.

[33] M. Jewginski, L. Fischer, C. Colombo, I. Huc, C. D. Mackereth, *ChemBioChem* **2016**, *17*, 727–736.

[34] S. A. Kang, P. J. Marjavaara, B. R. Crane, *J. Am. Chem. Soc.* **2004**, *126*, 10836–10837.

[35] H. Takashima, S. Shinkai, I. Hamachi, *Chem. Commun.* **1999**, 2345–2346.

[36] J. Muldoon, A. E. Ashcroft, A. J. Wilson, *Chem. A Eur. J.* **2010**, *16*, 100–3.

[37] M. H. Filby, J. Muldoon, S. Dabb, N. C. Fletcher, A. E. Ashcroft, A. J. Wilson, *Chem. Commun.* **2011**, *47*, 559–61.

[38] S. J. Turrell, M. H. Filby, A. Whitehouse, A. J. Wilson, *Bioorg. Med. Chem. Lett.* **2012**, *22*, 985–8.

[39] A. J. Wilson, J. R. Ault, M. H. Filby, H. I. A. Philips, A. E. Ashcroft, N. C. Fletcher, *Org. Biomol. Chem.* **2013**, *11*, 2206–12.

[40] J. Ohkanda, R. Satoh, N. Kato, *Chem. Commun.* **2009**, 6949–51.

[41] Y. Yamaguchi, N. Kato, H. Azuma, T. Nagasaki, J. Ohkanda, *Bioorg. Med. Chem. Lett.* **2012**, *22*, 2354–8.

[42] J. Ohkanda, *Chem. Rec.* **2013**, *13*, 561–75.

[43] S. Shinoda, H. Tsukube, *Chem. Sci.* **2011**, *2*, 2301.

[44] Y. Wei, G. L. McLendon, M. A. Case, C. B. Purring, T. Yu, A. D. Hamilton, Q. Lin, H. S. Park, C.-S. Lee, *Chem. Commun.* **2001**, 1580–1581.

[45] M. Mallon, S. Dutt, T. Schrader, P. B. Crowley, *ChemBioChem* **2016**, *17*, 774–783.

[46] Ayush Verma, and Joseph M. Simard, V. M. Rotello*, *Langmuir* **2004**, *20*, 4178–4181.

[47] H. Pelletier, J. Kraut, *Science (80-.).* **1992**, *258*, 1748–1755.

[48] A. Spencer, I. Evans, A. Spencer, G. Wilkinson, *J.C.S. Dalt.* **1973**, 204–209.

[49] J. E. Erman, G. C. Kresheck, L. B. Vitello, M. A. Miller, *Biochemistry* **1997**, *36*, 4054–4060.

[50] T. Y. Yonetani, *TEE J. Biol. Chem.* **1967**, *242*, 5008–5013.

[51] H. B. Bull, K. Breese, *Biochem. Biophys. Res. Commun.* **1966**, *24*, 74–78.

[52] L. B. Vitello, J. E. Erman, *Arch. Biochem. Biophys.* **1987**, *258*, 621–629.

[53] J. L. Res, B. B. Acta, B. B. Acta, B. B. Acta, *Biochemistry* **1976**, *15*, 1909–1914.

[54] G. W. Bushell, G. V Louie, G. D. Brayer, *J. Mol. Biol.* **1990**, *214*, 585–595.

[55] W. Liu, J. Rumbley, S. W. Englander, a J. Wand, *Protein Sci.* **2003**, *12*, 2104–2108.

[56] B. F. Van Gelder, E. C. Slater, *The Extinction Coefficient of Cytochrome c*, Elsevier, **1962**.

[57] E. Margoliash, N. Frohwirt, U. W. Riley, D. P. Phil, Tran8, 409 247a, S. Blackburn, A. G. Lowther, R. Cecil, A. G. Ogston, et al., *Biochem. J.* **1959**, *71*, 570–572.

FULL PAPER

Entry for the Table of Contents (Please choose one layout)

Layout 2:

FULL PAPER

Sarah H. Hewitt, Maria H. Filby, Ed Hayes, Lars T. Kuhn, Arnout P. Kalverda, Michael E. Webb and Andrew J. Wilson*
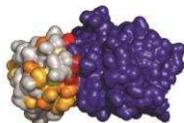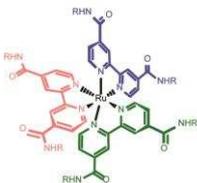
Ruthenium   *tris*(bipyridines) binding to cyt c acting as protein surface mimetics, including PPI inhibitions, further understanding of the binding interaction by looking at binding in many variable conditions, and NMR to probe where the binding site on cyt c is.